ACCSCIENCE PUBLISHING

International Journal of Systematic Innovation

ARTICLE

Identifying mineral potentials related to geological structures using deep learning

Hadi Shahraki[1]*, and Mohsen Jami[2]

[1]Department of Computer Engineering, Faculty of Industry and Mining, University of Sistan and Baluchestan, Khash, Sistan and Baluchestan, Iran

[2]Department of Mining, Faculty of Industry and Mining, University of Sistan and Baluchestan, Khash, Sistan and Baluchestan, Iran

Abstract

Artificial intelligence is increasingly being used as a powerful tool in various industries, including earth sciences. Geological structures play an undeniable role in the formation of mineral potentials. Investigating these structures relies on satellite imagery, together with expert interpretation, which can be a time-consuming process. Artificial intelligence can serve as a valuable tool to expedite this process and enhance the accuracy of mineral potential identification. This article presents a new model based on deep neural networks for identifying mineral potentials. The unique feature of the proposed method is the incorporation of morphological data alongside multispectral data to identify mineral potentials. To evaluate the effectiveness of the proposed method, advanced spaceborne thermal emission and reflection radiometer satellite images from a region in the southeast of Iran were utilized. The results demonstrate an improvement in the accuracy of the proposed method compared to similar approaches.

Keywords: Artificial intelligence; Deep learning; Deep neural network; Mineral potential identification; Machine learning

***Corresponding author:**
Hadi Shahraki
(Hadi_shahraki@eng.usb.ac.ir)

Citation: Shahraki H, Jami M. (2026). Identifying mineral potentials related to geological structures using deep learning. *Int J Systematic Innovation*. 10(1):11-18. https://doi.org/10.6977/IJoSI.202602_10(1).0002

Received: January 27, 2025

Revised: November 4, 2025

Accepted: January 5, 2026

Published online: February 13, 2026

Copyright: © 2026 Author(s). This is an Open-Access article distributed under the terms of the Creative Commons Attribution License, permitting distribution, and reproduction in any medium, provided the original work is properly cited.

Publisher's Note: AccScience Publishing remains neutral with regard to jurisdictional claims in published maps and institutional affiliations.

1. Introduction

Today, artificial intelligence, as a new technology, plays an important role in industries. Artificial intelligence can help improve processes and decisions by analyzing data to extract patterns and relationships that support decision-making. This can lead to an increase in productivity in various industries. Therefore, the use of artificial intelligence in various applications such as medicine (Chen *et al*., 2022), Internet of Things (Zhou *et al*., 2023), robotics (Soori *et al*., 2023), weather forecasting (Bochenek & Ustrnul, 2022), and intelligent vehicle systems (Suhaib *et al*., 2022) has grown significantly.

Artificial intelligence algorithms can also be used in geological and mineral mapping using multispectral satellite images (Shirmard, Farahbakhsh, Müller, *et al*., 2022). Oneof the most important advantages of using artificial intelligence in the preparation of geological maps is enhanced accuracy and speed of mapping (Sun *et al*., 2019), which has stimulated increased research in this area. Various algorithms have been used in geological and mineral mapping, including random forest (Kuhn *et al*., 2018; Radford

et al., 2018) support vector machine (SVM) (Cardoso-Fernandes *et al*., 2020; Othman & Gloaguen, 2014), and neural networks (Latifovic *et al*., 2018; Shirmard, Farahbakhsh, Heidari, *et al*., 2022).

The SVM is one of the most widely used algorithms in the preparation of geological maps (Cardoso-Fernandes *et al*., 2020; Othman & Gloaguen, 2014). Li *et al*. (2004) previously presented an automatic lithology classification method using advanced spaceborne thermal emission and reflection radiometer (ASTER) images using an SVM. Additionally, Bachri *et al*. (2019) reported a lithology classification method using this algorithm. Moreover, Bachri *et al*. (2019) and Cracknell & Reading (2014) compared different types of machine learning methods in the preparation of geological maps.

Neural networks are another widely used algorithm in the preparation of geological maps. Rigol-Sanchez *et al*. (2003) employed a neural network model to identify mineral potentials of gold in various areas in the southeast of Spain. Sergi *et al*. (1995) used neural networks to classify Landsat multispectral images. Moreover, Otele *et al*. (2021) used neural networks to prepare lithology maps.

The strong performance of deep learning or deep neural networks in various applications has led to the use of these methods in remote sensing processes (Ma *et al*., 2019). Additionally, deep learning algorithms have been used in the preparation of geological maps. Latifovic *et al*. (2018) utilized deep neural networks to accelerate the production of geological maps and increase their accuracy. Shirmard, Farahbakhsh, Heidari, *et al*. (2022) compared the performance of convolutional neural networks (CNNs) and SVMs, demonstrating that CNNs produce superior results compared to other methods.

In this study, a new deep learning method to identify mineral potentials is presented. Considering the importance of morphological data along with the multispectral data to identify mineral potentials, both types of data are used in the proposed method. For this purpose, the important features are first extracted from the morphological data and then used with the multispectral data to identify mineral potentials. The organization of this article is as follows: Section 2 introduces the proposed algorithm. Experimental results are reported in Section 3, and finally, Section 4 concludes the paper.

2. Methodology

In the proposed algorithm, prediction was made based on two categories of data: information related to multispectral data and morphological data.

A multispectral image is a collection of several image layers of an area, each of which is obtained in a specific wavelength band. For example, the ASTER satellite has the ability to create images with 14 different bands, in which nine are optical, and the rest are thermal. Six out of nine light bands produced by the ASTER satellite are called short-wave bands, and three other bands are visible. Multispectral data describe a feature vector for a pixel in a multispectral image. In geology, multispectral data can be used to identify different types of rocks and minerals based on their unique spectral signatures. This information can be used to identify areas of interest for mineral exploration and to map the distribution of minerals.

Petrological and morphological information are used by an expert to identify mineral potentials in remote sensing. Morphological data could provide information about the surface of the Earth, focusing on its terrain, elevation, and structural features. In this study, a band of multispectral satellite images is considered as a simple morphological snapshot of the Earth's surface.

Considering the importance of morphological and multispectral data, both were used in the proposed algorithm to identify mineral potentials. Because the morphological input is higher-dimensional than the multispectral data, the important features in the image containing the morphological data were first extracted. Subsequently, the extracted morphological features along with the multispectral data were combined and classified. In the proposed method, these steps were implemented using deep learning algorithms.

A multilayer perceptron (MLP) neural network, one of the most popular deep neural networks, consists of several layers, such as the input layer, the output layer, and the hidden layers. In the proposed method, this model was used for data classification.

Convolutional neural networks are also among the most commonly used models in deep learning methods, designed for processing grid-like data, such as images. The neurons in convolutional networks employ convolution operations on the input data. Convolution operations apply filters to input data to extract features from it. This can lead to the recognition of local patterns in the images, which can be used to recognize patterns and identify targets in the images. CNNs have been widely used in different applications. For this purpose, different models of these neural networks have been introduced, the most important of which are LeNet-5, AlexNet, VGGNet, ResNet, and convolutional self-encoder networks.

Convolutional autoencoder networks are deep learning models based on convolutional networks, which have attracted considerable attention in recent years due to their

ability to extract features from high-dimensional data, such as images. Convolutional autoencoder networks consist of two main components: an encoder and a decoder. In the first part of these networks, there is an encoder, which is responsible for compressing the input data, or in other words, extracting features from the input, while in the decoder part, the original input is reconstructed using the extracted features. In the proposed method, a convolutional autoencoder network was used to extract features from the morphological data.

In the proposed algorithm, to access the morphological data of each pixel, a neighborhood image with dimensions of 36 × 36 pixels was considered. To reduce the dimensions and extract important features from the image, a convolutional encoder was used. The details of the convolutional autoencoder network in the proposed algorithm are presented in Table 1. In the proposed algorithm, after training the encoder network, the encoder part was used to extract the features of the images. By using the convolutional encoder, the morphological data were reduced to 200 features. Then, the extracted morphological features along with the multispectral data for that pixel were put together and classified by an MLP network. In the output of the MLP network, each pixel was assigned to one of the desired classes. The parameters of the MLP network in the proposed algorithm are listed in Table 2. The general structure of the proposed algorithm is presented in Figure 1.

3. Results

In this study, multispectral satellite images of ASTER were used for mineral potential mapping. These images, presented in Shirmard, Farahbakhsh, Heidari, *et al.* (2022), are related to an area in the southeast of Iran, near Mirjaveh city, within the Sistan and Baluchestan province, with an area of about 66 km². The dimensions of the image are 513 × 577 pixels, with each pixel containing 225 m². In this image, nine different classes were considered, as shown in Figure 2. The details of this satellite image are mentioned in the study by Shirmard, Farahbakhsh, Heidari, *et al.* (2022). The pixels related to the nine classes were randomly divided into two parts: training and testing. A total of 70% of the pixels were considered as the training data and 30% as the test data. The training data were used in the learning process of the algorithms, which were then evaluated using the test data.

To clearly evaluate the performance of the proposed algorithm, it was compared with a conventional CNN model, which is one of the standard deep learning approaches widely used for lithological mapping. In addition, the results were also compared with two reference methods: the SVM, representing a traditional machine learning approach, and the MLP, representing a simple neural network model. This comparison followed the evaluation framework presented in Shirmard, Farahbakhsh, Heidari, *et al.* (2022). The distinctive advantage of the proposed model compared with the CNN approach lies in its ability to combine morphological features, extracted via a convolutional autoencoder, with multispectral information, allowing the network to capture both spectral and structural patterns.

We compared the proposed method with SVM, MLP, and CNN baselines reported by Shirmard, Farahbakhsh, Heidari, *et al.* (2022).

The results were compared using the overlap ratio of the sets (IOU), considering accuracy. The IOU criterion obtains the degree of overlap between the real pixels and the pixels predicted by the algorithms for class c, and calculates the accuracy of the percentage of pixels that are correctly segmented compared to the total pixels. These criteria are calculated as follows using Equations (1) and (2):

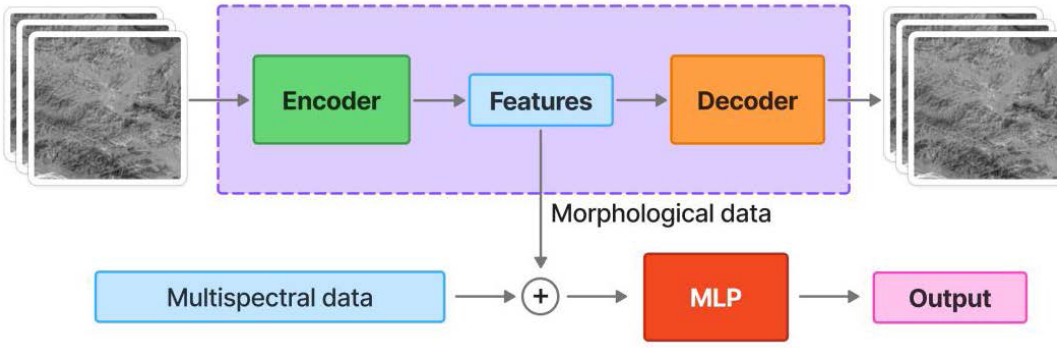

Figure 1. Outline of the proposed algorithm
Abbreviation: MLP: Multilayer perceptron.

Accuracy = The number of correct pixels/Total number of pixels (1)

IOU (c) = The number of pixels in the overlap area/The number of pixels in the union area (2)

Figure 3 shows the result of the proposed algorithm. The proposed algorithm was able to identify the mineral potentials presented in Figure 2 with high accuracy. Quantitative results obtained from the performance of the proposed algorithm, including IOU and accuracy criteria, are shown in Tables 3–5. Table 3 shows the accuracy value of different algorithms for the testing and training data. The proposed algorithm achieved the highest level of accuracy among the considered algorithms. Using the test data, the model achieved an accuracy 1.1 percentage points higher than that of the CNN algorithm.

For a more detailed comparison, the results of the IOU of different classes are shown in Tables 4 and 5. According to the results, the proposed algorithm exhibited superior performance to other algorithms. The proposed algorithm achieved its best performance in identifying class 8, with an IOU of 0.99 on the test data, significantly outperforming other comparable methods.

The obtained results demonstrate that integrating morphological and multispectral information significantly improved the accuracy of identifying mineral potential zones. This integration is crucial for practical mineral exploration applications, where field data acquisition is often time-consuming and expensive.

The proposed method can serve as an efficient tool for the preliminary identification of promising areas based on

Table 1. Details of the convolutional autoencoder network

Activation function	Window size	Number of filters	Type	Layer
ReLU	3 × 3	16	Conv2D	1
-	2 × 2	-	Max pooling 2D	2
ReLU	3 × 3	8	Conv2D	3
-	2 × 2	-	Max pooling 2D	4
ReLU	3 × 3	8	Conv2D	5
-	2 × 2	-	Max pooling 2D	6
ReLU	3 × 3	8	Conv2D	7
-	2 × 2	-	UpSampling2D	8
ReLU	3 × 3	8	Conv2D	9
-	2 × 2	-	UpSampling2D	10
ReLU	3 × 3	16	Conv2D	11
-	2 × 2	-	UpSampling2D	12
Sigmoid	3 × 3	1	Conv2D	13

Abbreviations: 2D: Two-dimensional; Conv: Convolutional; ReLU: Rectified linear unit.

Table 2. Hyperparameters of the multilayer perceptron neural network

Value	Hyperparameter
Rectified linear unit	Activation function
Adaptive moment estimation	Optimizer
15	Number of hidden layers
100	Number of hidden neurons
400	Epochs

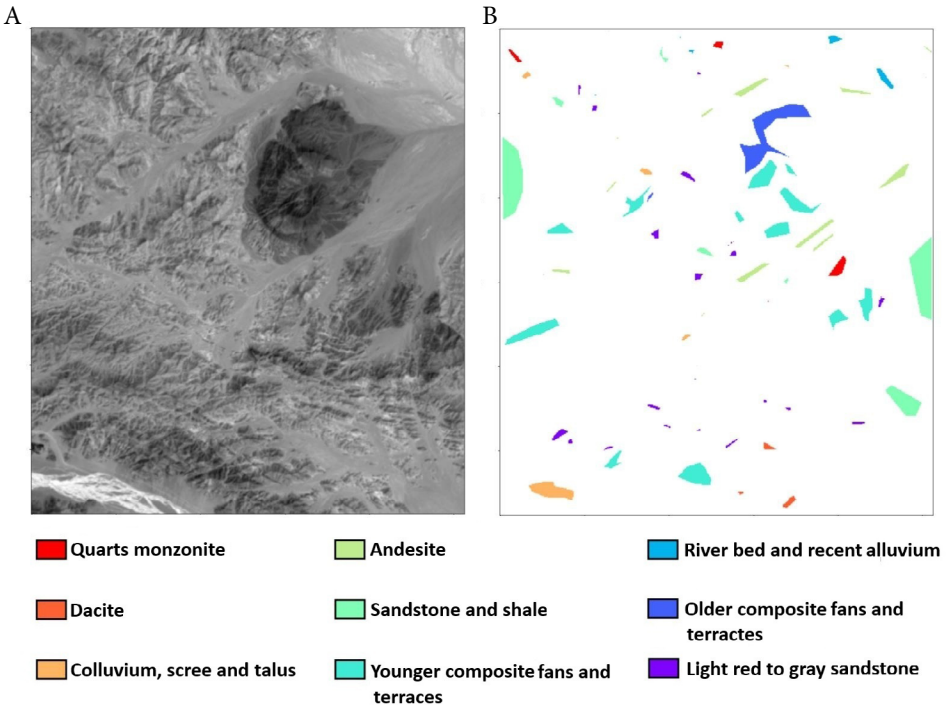

Figure 2. ASTER multispectral imagery and lithological information used for mineral potential analysis in the study area near Mirjaveh, southeastern Iran. (A) Satellite image related to the region in the southeast of Iran, along with the (B) mineral potentials in it. Images adapted from Shirmard, Farahbakhsh, Heidari, et al. (2022).

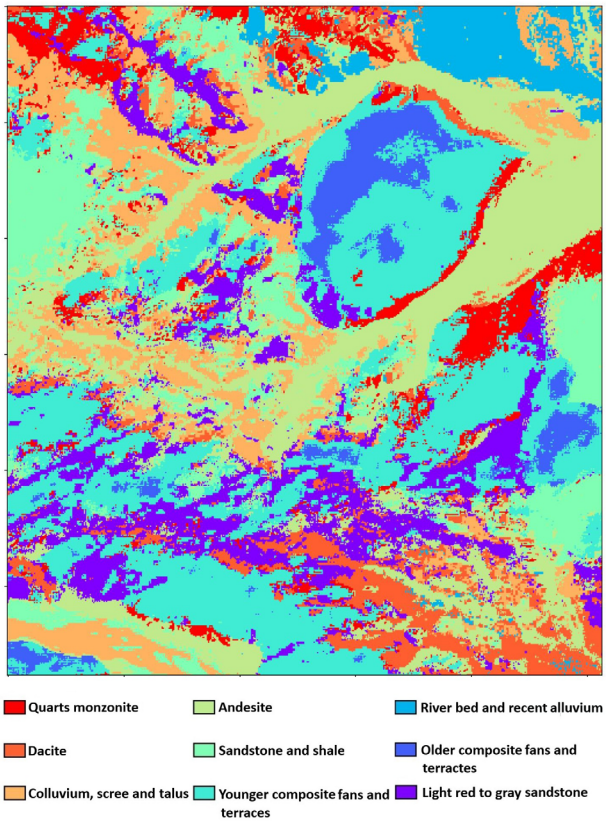

Figure 3. The result obtained using the proposed method to identify mineral potentials in Figure 2

Table 3. Comparison of the accuracy obtained from different methods

Proposed method	Convolutional neural network	Multilayer perceptron	Support vector machine	Data
99.4	98.2	96	94.6	Train
99.1	98	95.7	94.4	Test

Table 4. Comparison of the overlap ratio of the set values for different classes on the training data

Proposed method	Convolutional neural network	Multilayer perceptron	Support vector machine	Class
1.00	1.00	1.00	1.00	Class 1
0.99	0.99	0.94	0.93	Class 2
0.99	0.90	0.95	0.89	Class 3
0.99	0.96	0.92	0.90	Class 4
0.99	0.97	0.91	0.90	Class 5
0.97	0.94	0.88	0.84	Class 6
1.00	1.00	0.99	0.99	Class 7
0.99	0.77	0.79	0.60	Class 8
0.99	0.96	0.92	0.84	Class 9
0.99	0.94	0.92	0.87	Average

Table 5. Comparison of the overlap ratio of the set values for different classes on the test data

Proposed method	Convolutional neural network	Multilayer perceptron	Support vector machine	Class
0.99	1.00	0.99	0.99	Class 1
0.99	0.99	0.95	0.94	Class 2
0.95	0.85	0.97	0.90	Class 3
0.99	0.97	0.91	0.89	Class 4
0.98	0.97	0.91	0.89	Class 5
0.96	0.93	0.87	0.82	Class 6
0.99	1.00	0.99	1.00	Class 7
0.99	0.73	0.74	0.57	Class 8
0.99	0.97	0.91	0.83	Class 9
0.99	0.94	0.87	0.92	Average

satellite imagery, helping geologists concentrate their field investigations on the most prospective zones and thereby reducing both cost and time.

Moreover, the morphological feature extraction module, which captures structural and terrain characteristics of the Earth's surface, can be reused across different mineral exploration projects, as morphological patterns are not specific to any single mineral type. Consequently, for the exploration of other minerals or new geographic regions, only the multispectral data component of the model requires retraining using the new spectral datasets, while the morphological extractor can remain unchanged. This design makes the approach versatile and easily adaptable to various remote sensing-based geological mapping tasks.

4. Conclusion

This study presented a new method based on deep learning to identify mineral potentials and create lithology maps. The special feature of this algorithm is the use of morphological data in addition to the multispectral data. To use the morphological data, the features related to the neighboring image of each pixel were first extracted by an auto-encoder model, and then analyzed by an MLP neural network along with the multispectral data. The results obtained from the proposed algorithm were compared with those of three similar methods and outperformed the baseline methods. Future extensions could include uncertainty evaluation and testing the model across different geological regions to further assess its robustness and generalization capability.

Acknowledgments

None.

Funding

None.

Conflict of interest

The authors declare that they have no conflicts of interest.

Author contributions

Conceptualization: All authors
Formal analysis: All authors
Investigation: All authors
Methodology: All authors
Visualization: All authors
Writing–original draft: All authors
Writing–review & editing: All authors

Availability of data

The dataset used in this study was originally published by Shirmard *et al.* (2022) and is publicly available at https://github.com/sydney-machine-learning/deeplearning-lithology.

References

Bachri, I., Hakdaoui, M., Raji, M., Teodoro, A. C., & Benbouziane, A. (2019). Machine Learning Algorithms for Automatic Lithological Mapping Using Remote Sensing Data: A Case Study from Souk Arbaa Sahel, Sidi Ifni Inlier, Western Anti-Atlas, Morocco. *ISPRS International Journal of Geo-Information*, 8(6), 248.

https://doi.org/10.3390/ijgi8060248

Bochenek, B., & Ustrnul, Z. (2022). Machine Learning in Weather Prediction and Climate Anayses—Applications and Perspectives. *Atmosphere*, 13(2), 180.

https://doi.org/10.3390/atmos13020180

Cardoso-Fernandes, J., Teodoro, A. C., Lima, A., & Roda-Robles, E. (2020). Semi-Automatization of Support Vector Machines to Map Lithium (Li) Bearing Pegmatites. *Remote Sensing*, 12(14), 2319.

https://doi.org/10.3390/rs12142319

Chen, X., Wang, X., Zhang, K., Fung, K.-M., Thai, T. C., Moore, K., Mannel, R. S., Liu, H., Zheng, B., & Qiu, Y. (2022). Recent advances and clinical applications of deep learning in medical image analysis. *Medical Image Analysis*, 79, 102444.

https://doi.org/10.1016/j.media.2022.102444

Cracknell, M. J., & Reading, A. M. (2014). Geological mapping using remote sensing data: A comparison of five machine learning algorithms, their response to variations in the spatial distribution of training data and the use of explicit spatial information. *Computers & Geosciences*, 63, 22–33.

https://doi.org/10.1016/j.cageo.2013.10.008

Kuhn, S., Cracknell, M. J., & Reading, A. M. (2018). Lithologic mapping using Random Forests applied to geophysical and remote-sensing data: A demonstration study from the Eastern Goldfields of Australia. *Geophysics*, 83(4), B183–B193.

https://doi.org/10.1190/geo2017-0590.1

Latifovic, R., Pouliot, D., & Campbell, J. (2018). Assessment of Convolution Neural Networks for Surficial Geology Mapping in the South Rae Geological Region, Northwest Territories, Canada. *Remote Sensing*, 10(2), 307.

https://doi.org/10.3390/rs10020307

Li, D., Deogun, J., Spaulding, W., & Shuart, B. (2004). Towards Missing Data Imputation: A Study of Fuzzy K-means Clustering Method. In: *Rough Sets and Current Trends in Computing (Lecture Notes in Computer Science)*. Heidelberg: Springer Berlin Heidelberg, pp. 573–579.

https://doi.org/10.1007/978-3-540-25929-9_70

Ma, L., Liu, Y., Zhang, X., Ye, Y., Yin, G., & Johnson, B. A. (2019). Deep learning in remote sensing applications: A meta-analysis and review. *ISPRS Journal of Photogrammetry and Remote Sensing*, 152, 166–177.

https://doi.org/10.1016/j.isprsjprs.2019.04.015

Otele, C. G. A., Onabid, M. A., Assembe, P. S., & Nkenlifack, M. (2021). Updated Lithological Map in the Forest Zone of the Centre, South and East Regions of Cameroon Using Multilayer Perceptron Neural Network and Landsat Images. *Journal of Geoscience and Environment Protection*, 9(6), 120–134.

https://doi.org/10.4236/gep.2021.96007

Othman, A. A., & Gloaguen, R. (2014). Improving Lithological Mapping by SVM Classification of Spectral and Morphological Features: The Discovery of a New Chromite Body in the Mawat Ophiolite Complex (Kurdistan, NE Iraq). *Remote Sensing*, 6(8), 6867–6896.

https://doi.org/10.3390/rs6086867

Radford, D. D. G., Cracknell, M. J., Roach, M. J., & Cumming, G. V. (2018). Geological Mapping in Western Tasmania Using Radar and Random Forests. *IEEE Journal of Selected Topics in Applied Earth Observations and Remote Sensing*, 11(9), 3075–3087.

https://doi.org/10.1109/JSTARS.2018.2855207

Rigol-Sanchez, J. P., Chica-Olmo, M., & Abarca-Hernandez, F. (2003). Artificial neural networks as a tool for mineral potential mapping with GIS. *International Journal of Remote Sensing*, 24(5), 1151–1156.

https://doi.org/10.1080/0143116021000031791

Sergi, R., Solaiman, B., Mouchot, M. C., Pasquariello, G., & Posa, P. (1995). LANDSAT-TM image classification using principal components analysis and neural networks. In: Proceedings of the 1995 International Geoscience and Remote Sensing Symposium, IGARSS '95. Quantitative Remote Sensing for Science and Applications; 10–14 July 1995; Firenze, Italy. Volume 3, pp. 1927–1929.

https://doi.org/10.1109/IGARSS.1995.524069

Shirmard, H., Farahbakhsh, E., Heidari, E., *et al*. (2022). A Comparative Study of Convolutional Neural Networks and Conventional Machine Learning Models for Lithological Mapping Using Remote Sensing Data. *Remote Sensing*, 14(4), 819.

https://doi.org/10.3390/rs14040819

Shirmard, H., Farahbakhsh, E., Müller, R. D., & Chandra, R. (2022). A review of machine learning in processing remote sensing data for mineral exploration. *Remote Sensing of Environment*, 268, 112750.

https://doi.org/10.1016/j.rse.2021.112750

Soori, M., Arezoo, B., & Dastres, R. (2023). Artificial intelligence, machine learning and deep learning in advanced robotics, a review. *Cognitive Robotics*, 3, 54–70.

https://doi.org/10.1016/j.cogr.2023.04.001

Suhaib Kamran, S., Haleem, A., Bahl, S., Javaid, M., Prakash, C., & Budhhi, D. (2022). Artificial intelligence and advanced materials in automotive industry: Potential applications and perspectives. *Materials Today: Proceedings*, 62, 4207–4214.

https://doi.org/10.1016/j.matpr.2022.04.727

Sun, T., Chen, F., Zhong, L., Liu, W., & Wang, Y. (2019). GIS-based mineral prospectivity mapping using machine learning methods: A case study from Tongling ore district, eastern China. *Ore Geology Reviews*, 109, 26–49.

https://doi.org/10.1016/j.oregeorev.2019.04.003

Zhou, X., Hu, Y., Wu, J., Liang, W., Ma, J., & Jin, Q. (2023). Distribution Bias Aware Collaborative Generative Adversarial Network for Imbalanced Deep Learning in Industrial IoT. *IEEE Transactions on Industrial Informatics*, 19(1), 570–580.

https://doi.org/10.1109/TII.2022.3170149